Magneto-dynamic properties of Complex Oxide - $La_{0.7}Sr_{0.3}MnO_3/SrTiO_3$ - Heterostructure Interface

Suraj Singh[1], Torstein Bolstad[2], Ingrid Hallsteinsen[2,3], Thomas Tybell[2,4], and Erik Wahlström[1]

[1]Center for Quantum Spintronics, Department of Physics, NTNU - Norwegian University of Science and Technology, NO-7491 Trondheim, Norway

[2]Department of Electronic Systems, NTNU - Norwegian University of Science and Technology, NO-7491 Trondheim, Norway

[3]Advanced Light Source, Lawrence Berkeley National Laboratory, Berkeley, California 94720, USA

[4]Department of Materials Science and Engineering, University of Wisconsin-Madison, Madison, WI 53706, USA

We have studied the interface magnetodynamic properties of $La_{0.7}Sr_{0.3}MnO_3/SrTiO_3$ (111) heterostructures by Ferromagnetic resonance spectroscopy (FMR). In addition to the bulk FMR mode, the measurements indicate a mode originating from an independently excited ferromagnetic layer at the interface. The peak-to-peak intensity of the interface mode suggests a layer thickness in the order of few unit cells. Angle resolved FMR measurements reveal a hexagonal symmetry of the magneto-crystalline anisotropy of the mode with easy axis along the in-plane <1-10> crystallographic directions matching with the (111) surface orientation of the substrate, in contrast to bulk mode symmetry which is always found to have uniaxial symmetry caused by magnetostriction. The temperature dependence of the anisotropy, and a large temperature variation in the intensity ratio of interface and bulk mode indicates a coupling of the interface to the bulk mode.

The manganite-titanate interfaces have attracted a lot of attention for the novel physical properties driven by the structural, electronic and orbital reconstructions. A variety of interesting phenomena such as induced ferromagnetism, superconductivity, metal-insulator transition and multiferroics has been observed at such interfaces [1, 2]. The interface induced ferromagnetism in such systems is of fundamental interest, while at the same time the presence of the magnetic states confined to the interface opens new perspectives for 2D spintronics at oxide interfaces, and may have impact on spin dependent transport properties of novel spintronics devices such as magnetic tunnel junctions (TMJs)[3, 4]. In several (001) oriented manganite/titanate interface such as $LaMnO_3/SrTiO_3$ [5], $La_{0.7}Sr_{0.3}MnO_3/SrTiO_3$ [6] and $La_{0.7}Sr_{0.3}MnO_3/BaTiO_3$ [7] a Ti-induced interface ferromagnetism has been observed and is ascribed to orbital and spin reconstructions. An enhanced interlayer coupling has been reported at $La_{0.7}Sr_{0.3}MnO_3$ / $SrTiO_3$ (001) heterostructure due to the induced ferromagnetism which could improve the performance of $La_{0.7}Sr_{0.3}MnO_3/SrTiO_3$ TMJs [5]. The (111) oriented interfaces of such heterostructure are more prone to interface-induced emergent phenomena due to a terminating polar layer, where surface Ti atoms form a honeycomb lattice that hosts orbitals with hexagonal symmetry [2, 8]. However, detailed investigations of interface ferromagnetism in $La_{0.7}Sr_{0.3}MnO_3/SrTiO_3$ (111) interfaces are still missing. Investigation of such interfaces can thus give important information in order to develop a coherent understanding of the underlying physics and further their successful implementation in device applications.

The atomic layers close to the manganite-titanate interface are central for understanding this emergent phenomenon, and to elucidate their potential for spintronics applications. Studies of such buried interfacial layers using non-destructive techniques are advantageous over

techniques that involves sample cleavage. Ferromagnetic Resonance (FMR) spectroscopy is in this regard an interesting technique, exhibiting large sensitivity that should enable studies of magnetic interface properties of complex oxide heterostructures. To be observable as a separate interface mode the magnetic interface layer should preferably be weakly coupled to bulk ferromagnetic layer and display different magnetic properties than the bulk [9]. In manganites, the ferromagnetic ordering is often suppressed at the interface due to changes in the Mn^{3+}/Mn^{4+} ratio, where Mn^{3+} enriched layers have a decreased double exchange coupling [10, 11]. Hence, in such system exciting and detecting interface mode should be easier as compared to metallic ferromagnets where spins are tightly exchange coupled at an interface.

In this letter, we report the magnetodynamic properties of LSMO/STO (111) heterostructure using angle resolved FMR spectroscopy. We show that an interface mode in FMR spectra arises, connected to an interface ferromagnetic layer, from structural or electronic and orbital reconstructions. Further, we show how this mode can be used to extract some important properties of the LSMO/STO interface. The intensity observed indicates a sensitivity that well matches the expected signal from an interface layer thickness in the order of few unit cells. Moreover, the observed hexagonal symmetry of the mode shows that the magneto-crystalline anisotropy is dominant over the magnetostriction in contrast to the bulk mode that always found dominated uniaxial anisotropy caused by magnetostriction.

Epitaxial LSMO thin films were grown on (111)-oriented STO substrates by pulsed laser deposition from stoichiometric targets. Prior to deposition, the substrates were cleaned in deionized water at 70 °C in an ultrasonic bath, and then annealed for 1 h at 1050 °C in an oxygen

environment. The growth took place with an oxygen background pressure of 0.35 mbar and substrate temperature of 540 °C. The substrate to target separation was kept fixed at 45 mm. A KrF excimer laser (λ = 248 nm) with a fluency of 2 J.cm $^{-2}$ and repetition rate of 1 Hz was used to ablate the material from the target. After the deposition, the samples were cooled to room temperature at the rate of 15 K/min. The surface morphology was characterized by atomic force microscopy (AFM, Veeco Nanoscope V). The imaged step and terrace structure are consistent with films deposited on the vicinal substrate. More information on growth can be found elsewhere [12, 13]. The magnetic moment measurements were performed by Vibrating sample magnetometer (VSM). The in-plane magnetization hysteresis (M-H) loops measured at 50 K are shown in the fig. S5 of the suppl. Info. The thermo magnetization measurements (M-T) can be found elsewhere [14]. The magnetodynamic properties were studied by X-band Electron Paramagnetic Resonance (EPR/FMR) with fixed microwave frequency of 9.4 GHz (Bruker Bio-spin ELEXSYS 500, with a cylindrical TE-011 microwave cavity). The sample is attached to a quartz rod and mounted along the symmetry (z-axis) in the cylindrical cavity. The rod is attached to a goniometer allowing to rotate the sample 360° in-plane and out of plane. A microwave field is applied perpendicular to the sample plane in the cavity. The applied static magnetic field is then swept to record the FMR absorption. The FMR absorption are taken for 10, 15 and 30 nm LSMO thin films at various in-plane angle (ϕ), an angle between applied magnetic field and the [1-10] direction of the film, at precision of 2° shown in the fig. 1(a). The measurements were taken at room temperature as well as low temperature using liquid nitrogen cryostat.

The angle (ϕ) dependent in-plane FMR spectra acquired show that in contrast to a single FMR mode expected for ultrathin epitaxial films, all our samples display at least two similar modes

labeled as I_M and FMR [15], indicated by black arrows in the fig1(b), and Fig S1 of suppl. info. We focus on the mode I_M which is consistently found in all the investigated films and is a candidate for an interface mode. This mode displays a different symmetry than the uniform mode. To investigate the possible origin of this mode we have plotted the f (H) dispersion curve for various possible spin waves (see suppl. Info.) for an in-plane magnetized 15 nm LSMO thin film at room temperature in fig 2(b). The intersection of the spin wave dispersions with the measurement frequency (9.4 GHz) of the cavity FMR spectroscopy, shown as a horizontal line, relates to the possible resonance field of the corresponding modes. As shown in the fig 2(a), the resonance field of mode I_M is always found at higher fields than the FMR mode. Such a high field mode observed in in-plane FMR measurements can be ascribed to an exchange dominated surface mode due to surface spin pinning [16-18]. However, the mode is not found to follow the characteristics of surface modes (see suppl. Info.) [18-20] and hence a surface mode can be discarded. The frequency of perpendicular standing spin wave (PSSW), the first mode of the spin wave resonances is found too far away from the measurement frequency to be detected in our measurement geometry. The magnetostatic surface (MSSW) and the backward volume magnetostatic spin waves (BVMSW) excitation require a highly localized microwave field across the sample which is in contrast to uniform field in our cavity measurements [21]. Also, the resonance fields expected for these MSSW and BVMSW modes are not matching with the observed I_M's resonance field. Hence, they are also unlikely. Another more probable possibility is a layer that has an effective magnetization lower than the bulk. As can be seen, the dispersion curve for such a mode having effective magnetization (H_{eff} = 2500 Oe) approximately 32 ± 5 % smaller than the bulk plotted in solid pink line is matching well with the observed resonance field.

Hence, we refer the mode I_M, as a mode emerging from interface having a lower magnetization than the bulk of the thin film. This is in accordance to Bing et. al, who has previously reported such high resonance field mode as an interface mode [9]. However, impure inclusions in the film with different magnetic properties may also cause such a mode in FMR spectra. In order to exclude this possibility, out-of-plane FMR spectra, as shown in the fig. 2(c), was analyzed. The mode I_M is found to follow the behavior of the bulk mode, which indicates that it emerges from a thin planar geometry and not from impurities. Thus, the high resonance field appearance in all samples probed and the lower energy of the mode, compared to the bulk mode, clearly points towards I_M being an interface mode in contrast to exchange dominated surface modes which would have a much higher energy in such ultrathin films.

Furthermore, the ferromagnetic linewidth of the interface mode and peak to peak intensities were analyzed. The weak mode intensity prevents intensity and linewidth extraction from curve fitting. However, the mode is significant, and the trends are real and observable, so the peak-to-peak intensity and linewidths were measured. The linewidths are always found larger than that of the bulk mode as expected for the interface mode see fig. S4 in suppl. Info. The peak-to-peak intensity investigated from the FMR line shape is shown in the fig. 2(d). The FMR signal intensity depends on layer magnetization, film thickness and applied microwave power, fixed throughout the measurements [22, 23]. A quantitative analysis of the interface mode's intensity, points to an interfacial layer of order of few unit cells, in agreement with reported values for interface magnetism in the LSMO/STO system and is consistent with the mode originating from a very thin interfacial layer [6]. We note that the intensity ratio between the bulk and interface mode is in the order of 10^3 for all investigated films, varying with temperature as shown in fig.

2(d). The large temperature variation in intensity ratio indicates that interface mode is coupled to the bulk mode, albeit the coupling strength is decreasing with increasing temperature [23,24].

To further investigate the temperature dependence and coupling of the two modes we look at angle dependent measurements. It is evident from the angle dependent measurements (fig. 1(b)) that I_M display an hexagonal symmetry which match the LSMO/STO's (111) in-plane symmetry with easy axes along <1-10> crystallographic directions. Thus, the magnetic anisotropy of interface layer is firmly related to underlying crystal structure and is consistent with hexagonal magneto-crystalline anisotropy microscopically reported in LSMO/STO (111) [25-27]. However, the value of such huge anisotropy field observed is still not clear, interface induced complex processes may be responsible for this. In contrast to interface mode, the FMR mode is observed with uniaxial symmetry see fig S3 in suppl. Info, also found consistent with reported step edge induced uniaxial anisotropy [28-30]. Temperature dependent FMR measurements were acquired at a fixed in-plane orientation as depicted in the fig. 3(a) and 3(b) to explore this difference. A different temperature response is observed for I_M and the bulk mode. The angle resolved FMR measurements were repeated as a function of temperatures see fig S2 of suppl. info., and the effective magnetic anisotropy field, H_6 extracted from the difference between maximum and minimum resonance field for the interface mode is shown in the fig. 3(c). The FMR mode's anisotropy field, H_U however extracted from the fitting see fig S3 (a) and S3(b) and shown in fig. 3(d). The magnetic anisotropy field of both modes are found to increase with decrease in temperature, which could be due to approaching Curie temperature (T_C). However, such a huge change in magnetic anisotropy field for the interface mode, two orders of magnitude higher than that of bulk mode can not be solely explained by changes in T_C. One possibility is that the

anisotropy field of I_M is lowered due to a weaker coupling strength with increasing temperature. We also noticed an increase in mode intensity along <1-10> crystallographic directions in angle dependent FMR measurement see fig 1(b). This shows that the coupling strength has directional dependence and found maximum along easy direction [31].

There are different possible scenarios, which could be responsible for the magneto-dynamically active interface layer in such system. For example, there is a reported a-site cation mixing of 1-2 d_{111} layers at the interface [13], resulting in an effective (La,Sr)TiO3 layer at the substrate side. However, such compositions are not reported to be ferromagnetic [32]. Also, if a weakening of ferromagnetism due to a changed Mn^{3+}/Mn^{4+} ratio approaching the interface would be responsible then one would expect a stronger coupling to the bulk mode and no change in symmetry of the interface mode. Other possibilities includes interface-induced ferromagnetism either due to electronic reconstruction [2] or due to oxygen vacancies at interface [3]. Such processes result in a changed valence state of the Ti ions in STO at interface and thereby orbital and spin reconstructions, which generates a magnetic state at the interface [33]. However, it has been not reported in LSMO/STO (111) hence further measurements are required to confirm that Ti–induced ferromagnetism is responsible for the observed interface ferromagnetism.

In summary, we have studied the magnetodynamic properties of LSMO/STO heterostructure interface by angle resolved FMR. We found a weak low energy mode in the FMR spectra in addition to the bulk mode. Comparisons with calculations for the possible spin waves in the system indicates that the observed mode is an interface mode rather than an exchange or dipole surface spin waves. The mode intensity shows that the layer thickness is in the order of

few unit cells matching well with previous reports. The mode is found with hexagonal symmetry, matching with the LSMO/STO's (111) in-plane symmetry, in contrast to the bulk mode's symmetry, which is always found to have uniaxial symmetry. The anisotropy field of hexagonal symmetry is found highly temperature dependent. The decrease in magnetic anisotropy with increasing temperature for both modes points that the modes are coupled. Moreover, the intensity ratio of the modes, as well as the relative temperature dependence on the anisotropy field, is found decreasing with increasing temperature, which both indicate that the coupling strength is also seen to decrease with increasing temperature. These finding suggest that an interface ferromagnetic layer at LSMO/STO interface resulting from structural or orbital and spin reconstructions having a hexagonal magneto-crystalline anisotropy in contrast to the bulk mode symmetry. Taken together, this study shows that it is possible to induce and detect interface magneto-dynamic modes at oxide interfaces, opening a pathway for interface engineering of magnetic-dynamic systems for spintronics applications.

Acknowledgements

This work was partly supported by the Research Council of Norway through its Centre of Excellence funding scheme, project number 262633, "QuSpin". TT and TB acknowledge the Research Council of Norway for providing funding through Grant No. 231290. SS acknowledge partial funding obtained from the Norwegian PhD Network on Nanotechnology for Microsystems, which is sponsored by the Research Council of Norway, Division for Science, under contract no. 221860/F40.

References

1. H. Y. Hwang, Y. Iwasa, M. Kawasaki, B. Keimer, N. Nagaosa, and Y. Tokura Nature Mater.**11**, 103 (2012).
2. J. Chakhalian, A. J. Millis, and J. Rondinelli, Nat. Mater. **11**, 92 (2012).
3. Y. Suzuki, APL Materials **3**, 062402 (2015)
4. F. Y. Bruno, M. N. Grisolia, C. Visani, S. Valencia, M. Varela, R. Abrudan, J. Tornos, A. Rivera-Calzada, A. A. Ünal, S. J. Pennycook, Z. Sefrioui, C. Leon, J. E. Villegas, J. Santamaria, A. Barthélémy, and M. Bibes, Nat. Commun. **6**, 6306 (2015).
5. J. Garcia-Barriocanal, J. C. Cezar, F. Y. Bruno, P. Thakur, N. B. Brookes, C. Utfeld, A. Rivera-Calzada, S. R. Giblin, J. W. Taylor, J. A. Duffy, S. B. Dugdale, T. Nakamura, K. Kodama, C. Leon, S. Okamoto, and J. Santamaria, Nat. Commun.**1**, 82 (2010).
6. F. Y. Bruno, J. Garcia-Barriocanal, M. Varela, N. M. Nemes, P. Thakur, J. C. Cezar, N. B. Brookes, A. Rivera-Calzada, M. Garcia-Hernandez, C. Leon, S. Okamoto, S. J. Pennycook, and J. Santamaria, Phys. Rev. Lett. **106**, 147205 (2011).
7. Y. Liu, J. Tornos, S. G. E. te Velthuis, J. W. Freeland, H. Zhou, P. Steadman, P. Bencok, C. Leon, and J. Santamaria, APL Mater.**4**, 46105 (2016).
8. D. Doennig, W. E. Pickett, and R. Pentcheva, Phys. Rev. Lett. **111**, 126804 (2013).
9. P. C-bing and D. D-sheng, J. Magn. Magn. Mater. **114**, 249 (1992).
10. J. S. Lee, D. A. Arena, P. Yu, C. S. Nelson, R. Fan, C. J. Kinane, S. Langridge, M. D. Rossell, R. Ramesh, and C. C. Kao, Phys. Rev. Lett.**105**(25), 257204 (2010).

11. A. Tebano, C. Aruta, S. Sanna, P. Medaglia, G. Balestrino, A. Sidorenko, R. De Renzi, G. Ghiringhelli, L. Braicovich, V. Bisogni, and N. Brookes, Phys. Rev. Lett. **100** (13), 137401 (2008).
12. I. Hallsteinsen, J. E. Boschker, M. Nord, S. Lee, M. Rzchowski, P. E. Vullum, J. K. Grepstad, R. Holmestad, C. B. Eom, and T. Tybell, J. Appl. Phys. **113**(18), 183512 (2013).
13. I. Hallsteinsen, M. Nord, T. Bolstad, P.-E. Vullum, J. E. Boschker, P. Longo, R. Takahashi, R. Holmestad, M. Lippmaa, and T. Tybell, Cryst. Growth Des. **16**, 2357 (2016).
14. V. Flovik, F. Macià, S. Lendínez, J. M. Hernàndez, I. Hallsteinsen, T. Tybell and E. Wahlström J. Magn. Magn. Mater.**420** 280 (2016).
15. A. K. Pradhan, J. B. Dadson, D. Hunter, K. Zhang, S. Mohanty, E. M. Jackson, B. Lasley-Hunter, K. Lord, T. M. Williams, R. R. Rakhimov, J. Zhang, D. J. Sellmyer, K. Inaba, T. Hasegawa, S. Methews, B. Joseph, B. R. Sekhar, U. N. Roy, Y. Cui, and A. Burger, J. Appl. Phys. **100**, 033903 (2006).
16. J. T. Yu, R. A. Turk, and P. E. Wigen, Phys. Rev. B **11**, 420 (1975).
17. Y.-L. Zhao, Y. Sun, L.-Q. Pan, K.-S. Li and D.-B. Yu, Appl. Phys. Lett. **102**, 042404 (2013).
18. H. Puszkarski, Prog. Surf. Sci. **9**, 191 (1979).
19. C. Kittel, Phys. Rev. **110**, 1295 (1958).
20. X. Liu, Y. Zhou, and J. Furdyna, Phys. Rev. B **75**, 195220 (2007).
21. V. Flovik, F. Maciá, A. D. Kent, and E. Wahlström, J. Appl. Phys. **117**, 143902 (2015).
22. Y.-C. Chen, D.-S. Hung, Y.-D. Yao, S.-F. Lee, H.-P. Ji, and C. Yu, J. Appl. Phys. **101**, 09C104 (2007)

23. A. Layadi and J. O. Artman, J. Magn. Magn. Mater.**92**, 154 (1990), J. Magn. Magn. Mater.**176**, 175 (1997).

24. H. Puszkarski, Phys. Stat. Sol (b) **171**, 205 (1992).

25. I. Hallsteinsen, E. Folven, F.K. Olsen, R.V. Chopdekar, M.S. Rzochowski, C.B. Eom, J.K. Grepstad, and T. Tybell, APL mater. **3**, 062501 (2015).

26. P. K. Rout, I. Agireen, E. Maniv, M. Goldstein, and Y. Dagan, Phys. Rev. B 95, 241107(R) (2017)

27. L. Miao, R. Du, Y. Yin, and Q. Li, Appl. Phys. Lett. 109, 261604 (2016).

28. M. Mathews, F. M. Postma, J. C. Lodder, R. Jansen, G. Rijnders, and D. H. A. Blank, Appl. Phys. Lett. **87**, 242507 (2015).

29. P. Perna, C. Rodrigo, E. Jiménez, F. J. Teran, N. Mikuszeit, L. Méchin, J. Camarero, and R. Miranda, J. Appl. Phys. **110**, 013919 (2011).

30. T. Bolstad, E. Lysne, U. L. Österberg, and T. Tybell, "Thickness dependent uniaxial magnetic anisotropy due to step-edges in (111)-oriented La0.7Sr0.3MnO3 thin films" submitted to J. Magn. Magn. Mater.

31. B. Heinrich, J. F. Cochran, M. Kowalewski, J. Kirschner, Z. Celinski, A. S. Arrott, and K. Myrtle, Phys. Rev. B **44**, 9348 (1991).

32. Joseph E. Sunstrom, Susan M. Kauzlarich, and Peter Klavins. Synthesis, structure and properties of $La_{1-X}Sr_XTiO3$ ($0 \leq x \leq 1$). Chemistry of Materials, **4** 346–353, 1992.

33. N. Pavlenko, T.Kopp, E. Y. Tsymbal, J. Mannhart and G. A. Sawatzky, Phys. Rev. B **86** 064431 (2012).

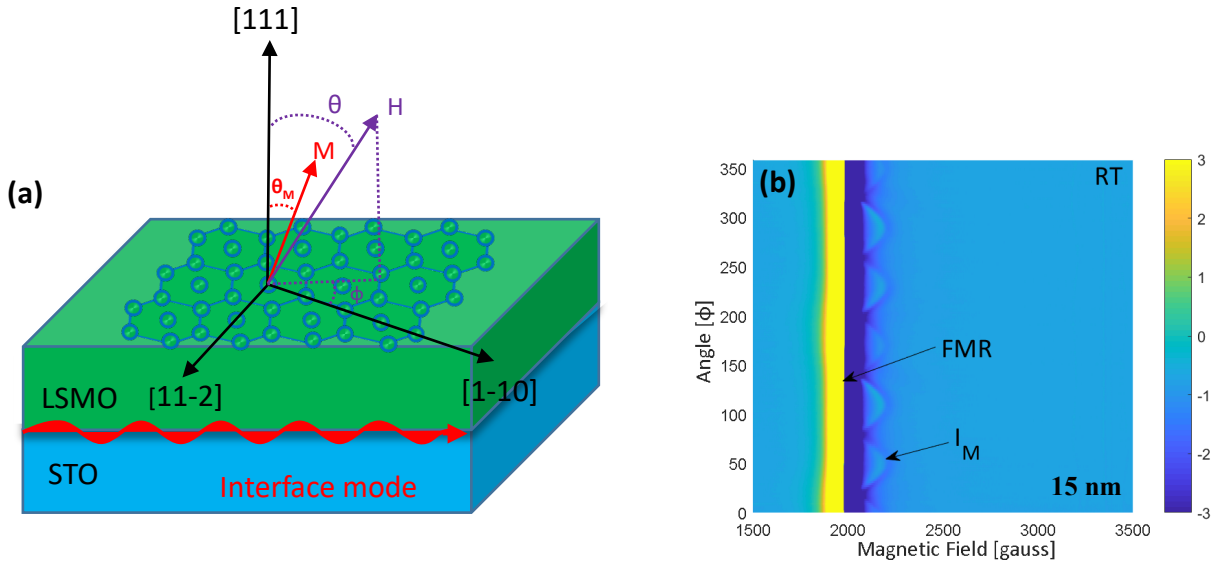

Fig 1(a) *shows the schematic of LSMO/STO heterostructure having hexagonal in-plane symmetry. Azimuthal angle (ϕ) dependent X-band 2D-FMR spectra of LSMO 15 nm at RT in fig.* ***1(b)****. Black arrows in the figure indicate the detected modes.*

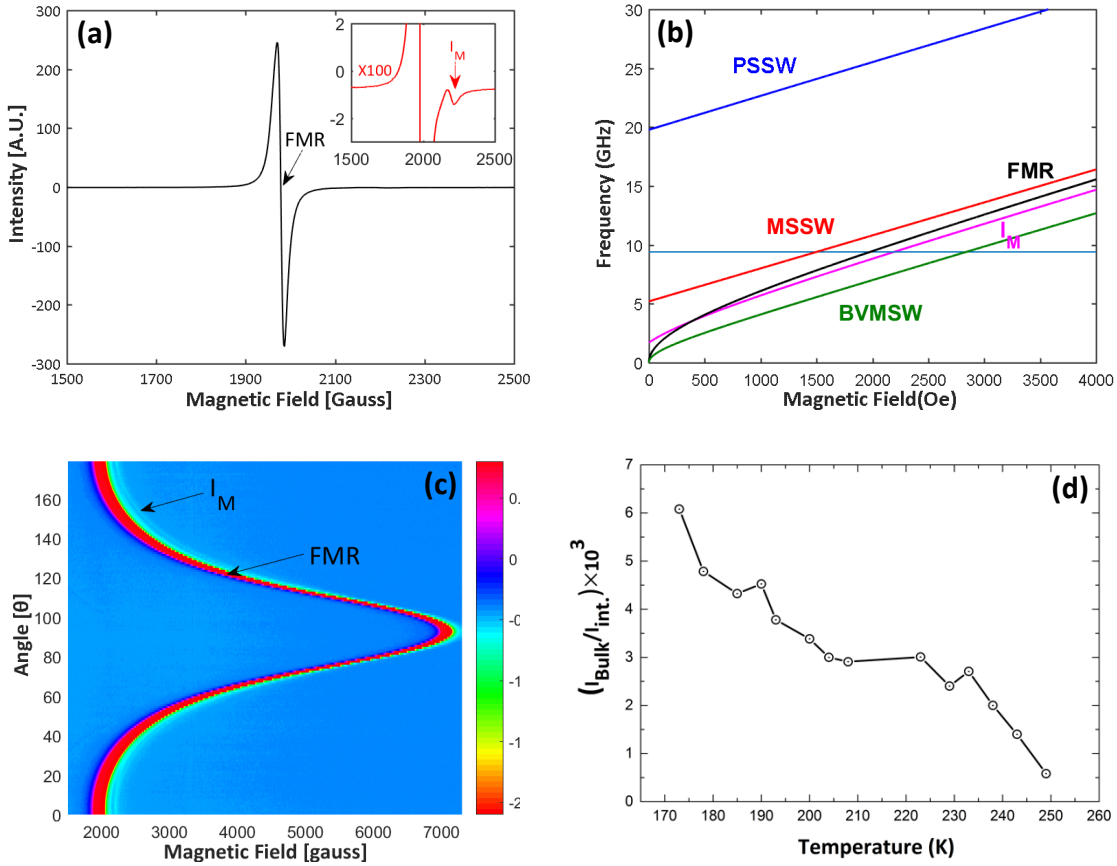

*Fig.2**(a):** The FMR absorption spectra taken at a fixed in-plane magnetic field from 15 nm film. The figure in the inset shows the zoomed y scale of the fig 2(a). The interface mode is indicated by red arrow . **2(b)**: The f (H) dispersion curve plotted for the perpendicular standing spin wave (PSSW), magnetostatic surface spin wave (MSSW), backward volume surface spin wave, uniform mode (FMR) & interface mode (I_M) and are shown by solid blue, red, green black and pink lines respectively. The pink curve shows the dispersion curve for an interface mode having effective magnetization lower than the bulk mode. The cyan horizontal line shows the measurement frequency (9.4 GHz) of cavity FMR spectroscopy. **2(c)**: The polar angle (θ) dependent 2D-FMR spectra of 15 nm film taken at RT. **2(d):** The intensity ratio of bulk and interface mode shown against temperature. The decrease in the intensity ratio with increasing temperature indicates a decrease in coupling of interface mode to the bulk.*

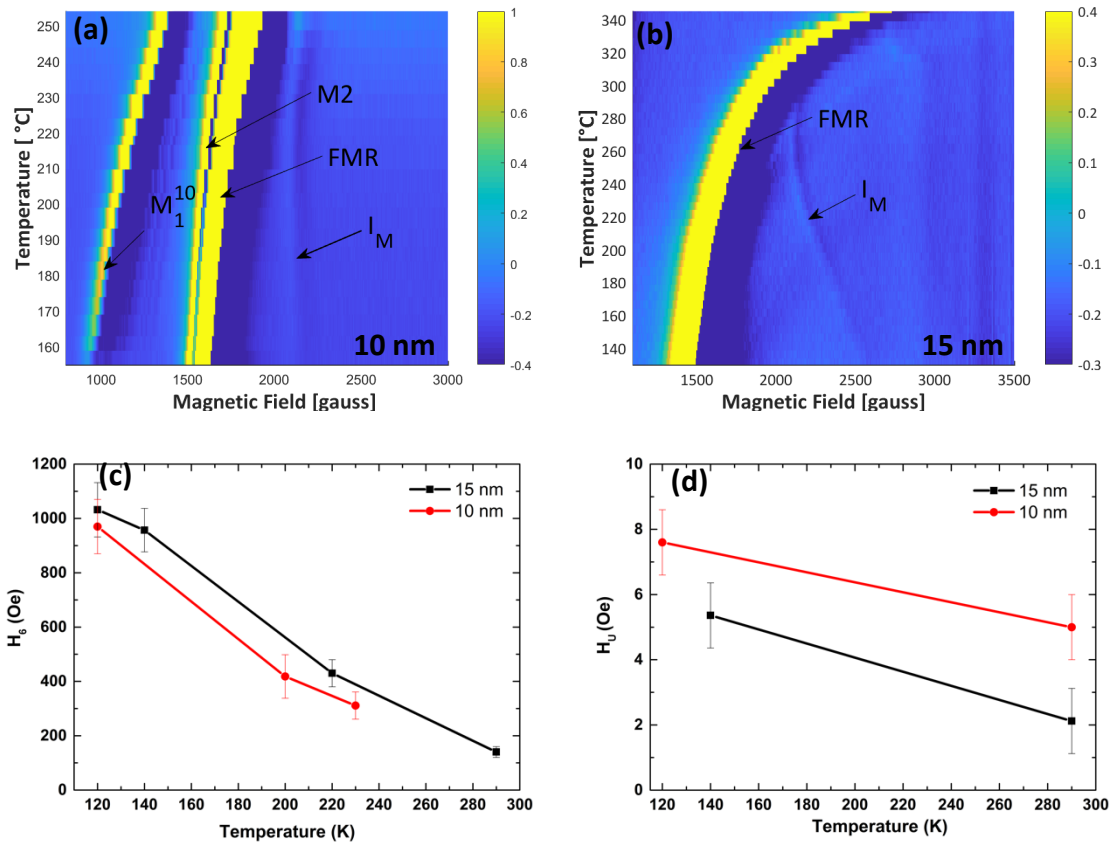

Fig. 3 *Temperature dependent FMR spectra of LSMO 10 fig* ***3(a)*** *and 15 nm fig* ***3(b)*** *at fixed in-plane magnetic field orientation. The magnetic anisotropy fields H_6 and H_U extracted for the interface and bulk mode from the in-plane angle (ϕ) dependent FMR measurements at different temperatures for 10 and 15 nm films in fig* ***3(c)*** *and* ***3 (d)*** *respectively.*

Supplementary information for Magneto-dynamic properties of Complex Oxide - $La_{0.7}Sr_{0.3}MnO_3/SrTiO_3$ - Heterostructure Interface

Suraj Singh[1], Torstein Bolstad[2], Ingrid Hallsteinsen[2,3], Thomas Tybell[2,4], and Erik Wahlström[1]

[1]Center for Quantum Spintronics, Department of Physics, NTNU - Norwegian University of Science and Technology, NO-7491 Trondheim, Norway

[2]Department of Electronic Systems, NTNU - Norwegian University of Science and Technology, NO-7491 Trondheim, Norway

[3]Advanced Light Source, Lawrence Berkeley National Laboratory, Berkeley, California 94720, USA

[4]Department of Materials Science and Engineering, University of Wisconsin-Madison, Madison, WI 53706, USA

Angle dependent FMR measurements at room temperature

Fig. S1 shows the angle resolved FMR measurements of 10 nm and 30 nm LSMO films at RT. In addition to FMR and I_M mode mentioned in the letter, other observed modes are labelled as mode M_1^{10}, M2, and M3 and indicated by black arrows. The mode M_1^{10}, where superscript shows the film thickness, is observed in only 10 nm and the mode M3 in 15 nm and 30 nm respectively. The modes M2, I_M and FMR mode are observed in all the investigated films.

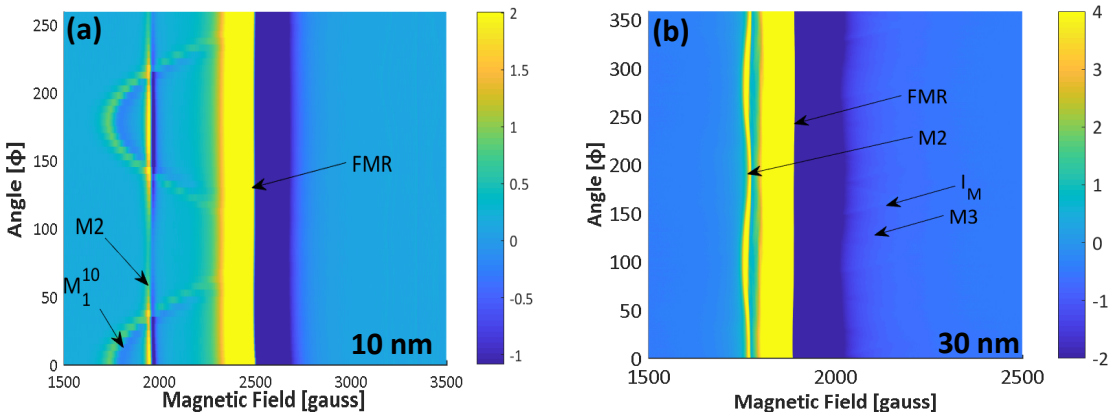

Fig. S1 Angle resolved FMR measurements at RT for 10 and 30 nm LSMO films.

Angle dependent FMR measurements at various temperatures

Angle resolve FMR measurements for different temperatures for 10 and 15 nm films are shown in the fig S2. It was found that the magneto-crystalline anisotropy field of the hexagonal symmetry decreases with increasing temperature.

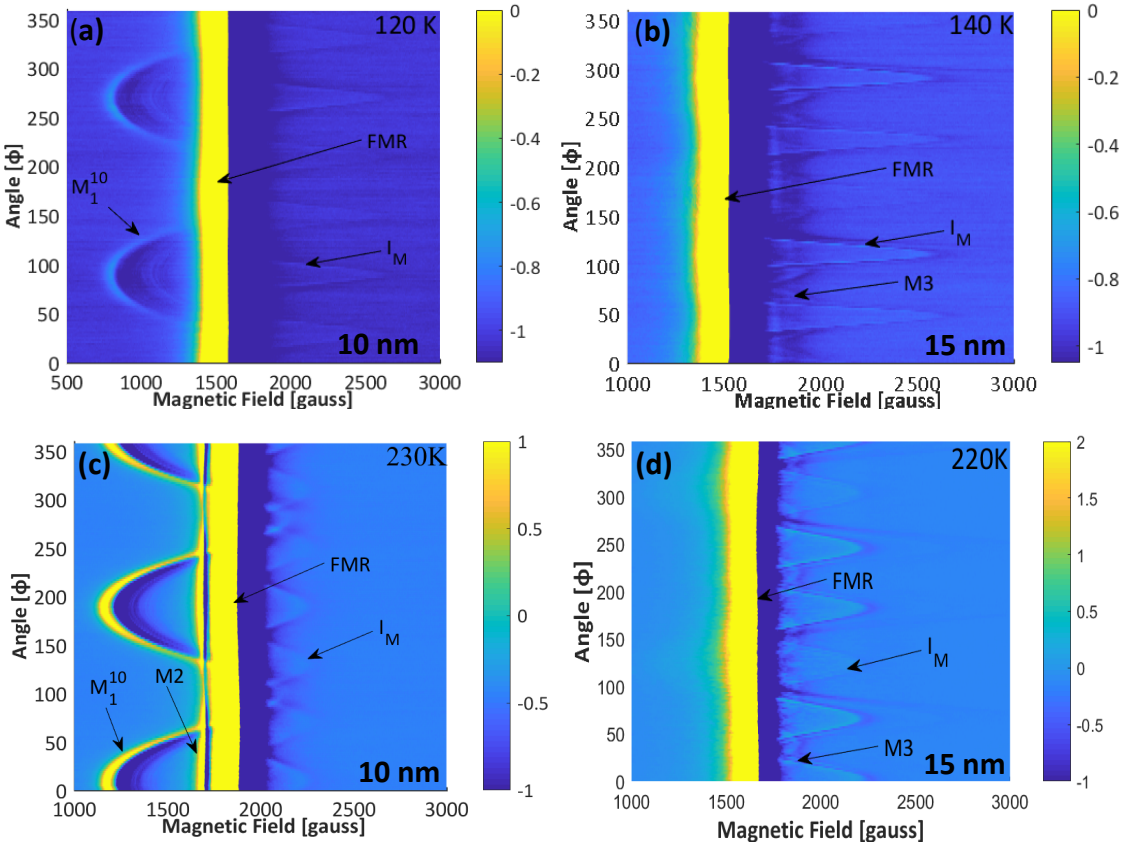

Fig. S2 Angle resolved FMR measurement of LSMO 10 nm in fig S2 (a), S2 (c) and 15 nm in fig S2 (b), S2 (d) at the temperatures mentioned at right top corner of each fig.

Extracting FMR mode's magnetic anisotropy field

The ferromagnetic resonance field of FMR mode was extracted after fitting the FMR absorption to the sum of derivative of symmetric and antisymmetric Lorentzian functions [8]. The extracted resonance fields at various in-plane angle (ϕ) were then fitted to equation (1) to extract the anisotropy field, see fig. S3(a), and S3(b).

$$f = f_0 + A\sin 2(\phi - \phi_A) + B\sin 4(\phi - \phi_B) + C\sin 6(\phi - \phi_C) \quad (1)$$

where, f_0, *A, B and C* are fitting parameters. ϕ_A, ϕ_B and ϕ_C are the phase shifts. The values of the B, and C are found very small hence neglected. The value 2A which gives the uniaxial anisotropy field is shown in the fig. 3 (d)

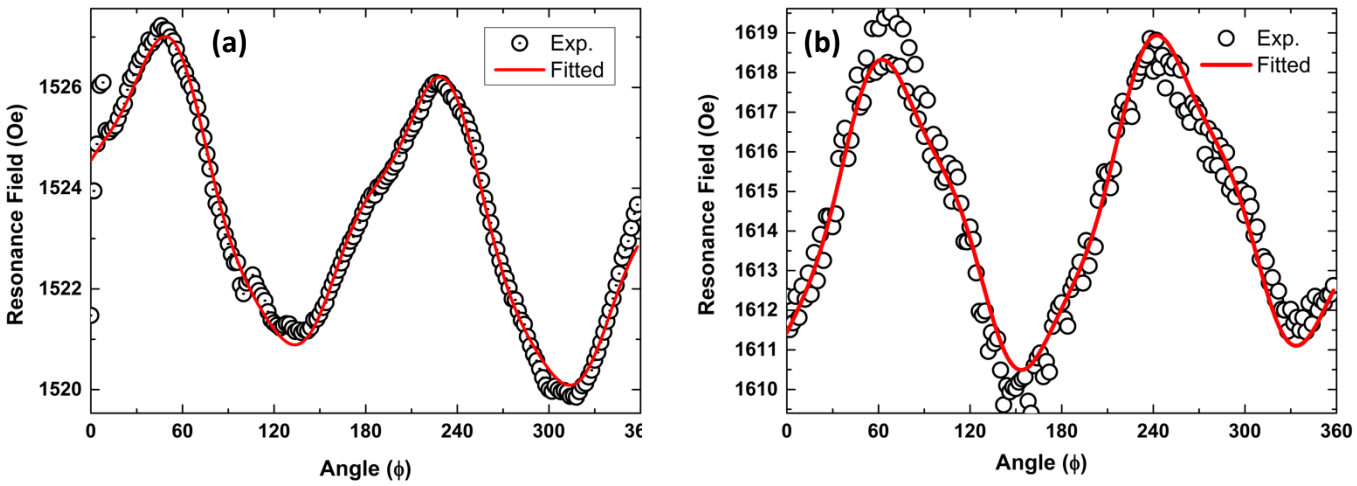

Fig. S3 Angle dependent ferromagnetic resonance field extracted after fitting the FMR line shape for 15 nm film at 140K fig S3 (a) and for 10 nm at 120K fig S3 (b). The plot shows the uniaxial anisotropy for the mode.

Peak to peak linewidth

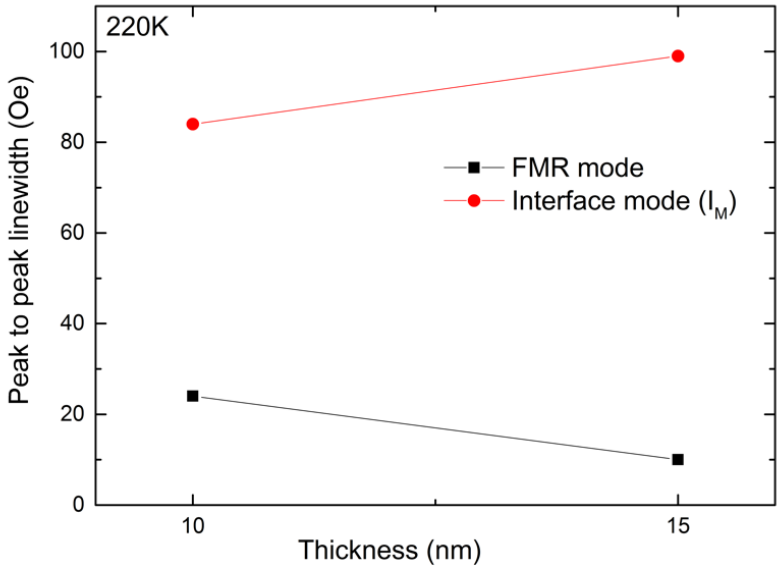

Fig. S4 The peak-to-peak linewidth measured for the FMR mode and interface mode for 10 and 15 nm films at 220K

In-plane hysteresis loops of samples at 50K

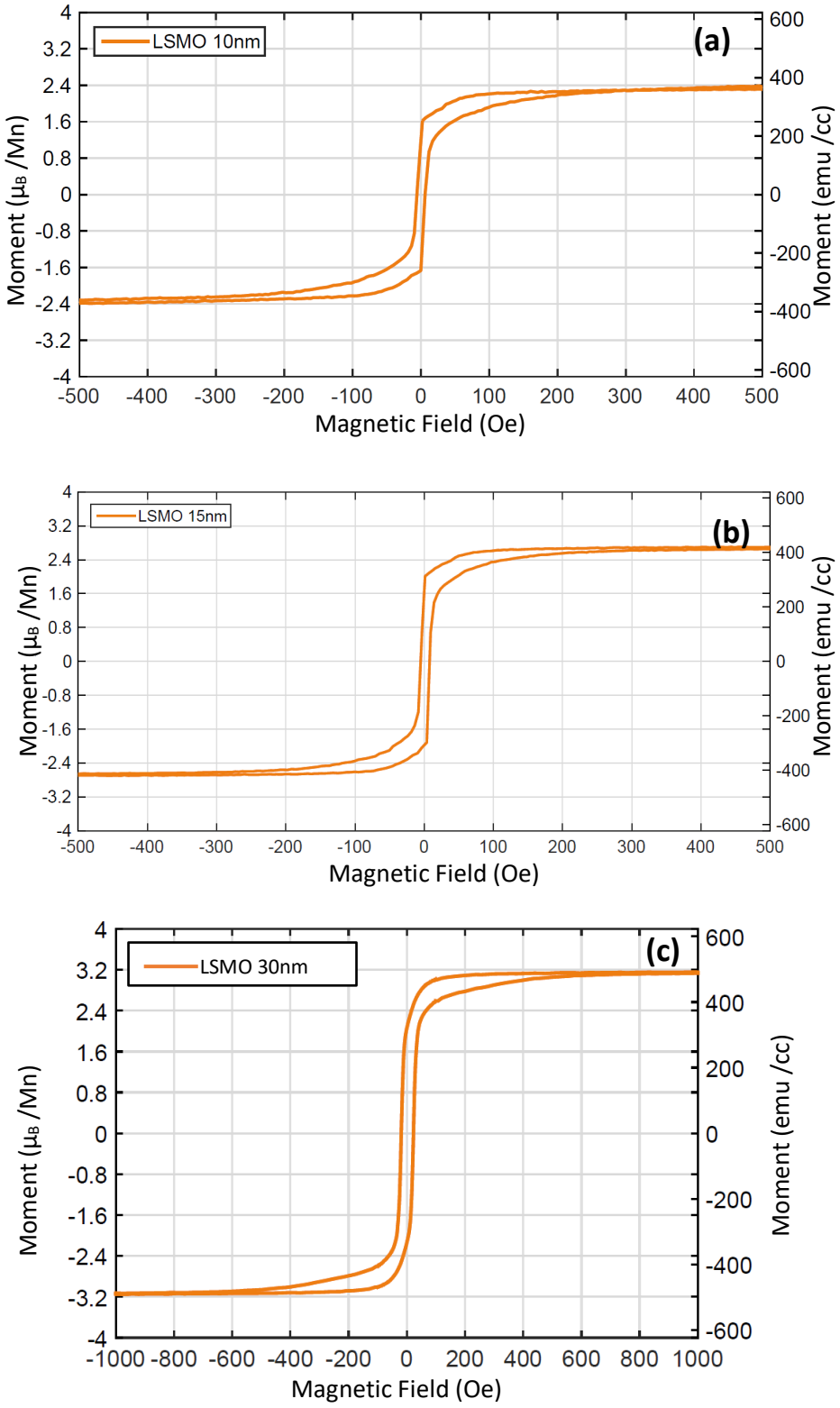

Fig. S5 The M-H loop of 10, 15 and 30 nm thin films measured by Quantum design Vibrating sample magnetometry at 50K.

Analysis of spin other possible spin waves:

To elucidate if the I_M data fit a surface mode we have also considered the Puszkarski's surface inhomogeneity (SI) model [2]. According to this model, surface spins are tightly pinned due to the surface anisotropy which results in excitation of perpendicular spin waves (PSSW), or spin wave resonances (SWR), whose n^{th} mode is given by the Kittel relation [3]

$$H_n = H_0 - n^2 \frac{D}{g\mu_B}\frac{\pi^2}{d^2} \quad (2)$$

where, H_0 is the position of the theoretical uniform mode, D is the exchange stiffness, and its value for LSMO is 144 meV·Å^2, and $D/g\ \mu_B$ = 12.42 T·nm^2. Based on equation (2), the difference between the uniform mode and the first surface mode is large, around 5440 Oe for a 15 nm thick film. We note that this range falls outside of our measurement limit, and hence cannot be observed in our set-up. Hence, as I_M is observed close to the FMR mode, the possibility of the I_M mode to be a member of SWR due to spin pinning is very low. We have also analyzed the angular dependence of the extra (I_M)mode - spin wave resonances exhibit a critical angle in in-plane and out-of-plane rotation measurements. This occurs when all modes merge into a single mode. As magnetic field's direction is tilted away from this critical angle, the first body mode transformed to surface mode and vice-versa [1,4]. The mode I_m doesn't show any such characteristics. We accordingly conclude that the mode I_M is not a spin wave resonances or a surface mode.

Spin wave dispersion relations used

The following relations have been used to plot the dispersion curves [5-7]:

$$f = \frac{\gamma}{2\pi}\sqrt{H_r(H_r + H_{eff})} \qquad \text{Kittel}$$

$$f = \frac{\gamma}{2\pi}\sqrt{(H_r + Dk^2)(H_r + H_{eff} + Dk^2)} \qquad \text{PSSW}$$

$$f = \frac{\gamma}{2\pi}\sqrt{H_r(H_r + H_{eff}) + H_{eff}^2\left(\frac{1 - e^{-2k\prime d}}{4}\right)} \qquad \text{MSSW}$$

$$f = \frac{\gamma}{2\pi}\sqrt{H_r\left(H_r + H_{eff}\left(\frac{1 - e^{-k\prime d}}{k'd}\right)\right)} \qquad \text{BVMSW}$$

Here, f is frequency of the cavity, γ is the gyromagnetic ratio, where γ/2π ≈ 28 GHz/T, H_r is resonance field, d is the thickness, k = n π/d, n is an odd integer assuming symmetric boundary condition for LSMO, and $k' \approx \pi/d$, and $H_{eff} = 4\pi M_S$ is effective field, The value of H_{eff} =3720 Oe has been used which was extracted from the room temperature FMR data.

The Kittel or uniform excitation mode (k = 0) is always excited in the system and labelled as FMR mode. The perpendicular standing spin wave (PSSW) which is the first mode of above-mentioned Kittel relation (eq. 2) and has already been discussed. The frequency of this mode is very high, and it will thus not intersect the measurement frequency and cannot be detected in our measurements (see fig 2(b). Further, magnetostatic surface (MSSW) and the backward volume magnetostatic spin waves (BVMSW) excitation requires a highly localized microwave field across the sample which is in contrast to uniform field in our cavity measurements [8].

References

1. X. Liu, Y. Zhou, and J. Furdyna, Phys. Rev. B **75**, 195220 (2007).
2. H. Puszkarski, Prog. Surf. Sci. 9, 191 (1979).
3. C. Kittel, Phys. Rev. **110**, 1295 (1958)
4. J. T. Yu, R. A. Turk, and P. E. Wigen, Phys. Rev. B **11**, 420 (1975).
5. C. Kittel Phys. Rev. **73**, 155 (1948).
6. R. Damon and J. Eshbach, Phys. Rev **118**, 1208 (1960).
7. B. A. Kalinikos, IEE Proc. H **127**, 4 (1980).
8. V. Flovik, F. Maciá, A. D. Kent, and E. Wahlström, J. Appl. Phys. **117**, 143902 (2015).